Outer Membrane Protein A of *Escherichia coli* Inserts and Folds into Lipid Bilayers by a Concerted Mechanism[†]

Jörg H. Kleinschmidt,[‡] Tanneke den Blaauwen,[§] Arnold J. M. Driessen,[§] and Lukas K. Tamm*,[‡]

Department of Molecular Physiology and Biological Physics and Center for Structural Biology, University of Virginia Health Sciences Center, P.O. Box 10011, Charlottesville, Virginia 22906-0011, and Department of Microbiology, University of Groningen, Kerklaan 30, 9751 NN Haren, The Netherlands

ABSTRACT: Unfolded outer membrane protein A (OmpA) of *Escherichia coli* spontaneously inserts and refolds into lipid bilayers upon dilution of denaturing urea. In the accompanying paper, we have developed a new technique, time-resolved distance determination by fluorescence quenching (TDFQ), which is capable of monitoring the translocation across lipid bilayers of fluorescence reporter groups such as tryptophan in real time [Kleinschmidt, J. H., and Tamm, L. K. (1999) *Biochemistry 38*, 4996−5005]. Specifically, we have shown that wild-type OmpA, which contains five tryptophans, inserts into lipid bilayers via three structurally distinct membrane-bound folding intermediates. To take full advantage of the TDFQ technique and to further dissect the folding pathway, we have made five different mutants of OmpA, each containing a single tryptophan and four phenylalanines in the five tryptophan positions of the wild-type protein. All mutants refolded *in vivo* and *in vitro* and, as judged by SDS−PAGE, trypsin fragmentation, and Trp fluorescence, their refolded state was indistinguishable from the native state of OmpA. TDFQ analysis of the translocation across the lipid bilayer of the individual Trps of OmpA yielded the following results: Below 30 °C, all Trps started from a far distance from the bilayer center and then gradually approached a distance of approximately 10 Å from the bilayer center. In a narrow temperature range between 30 and 35 °C, Trp-15, Trp-57, Trp-102, and Trp-143 were detected very close to the center of the lipid bilayer in the first few minutes and then moved to greater distances from the center. When monitored at 40 °C, which resolved the last steps of OmpA refolding, these four tryptophans crossed the center of the bilayer and approached distances of approximately 10 Å from the center after refolding was complete. In contrast Trp-7 approached the 10 Å distance from a far distance at all temperatures and was never detected to cross the center of the lipid bilayer. The translocation rates of Trp-15, Trp-57, Trp-102, and Trp-143 which are each located in different outer loop regions of the four β-hairpins of the eight-stranded β-barrel of OmpA were very similar to one another. This result and the common distances of these Trps from the membrane center observed in the third membrane-bound folding intermediate provide strong evidence for a synchronous translocation of all four β-hairpins of OmpA across the lipid bilayer and suggest that OmpA inserts and folds into lipid bilayers by a concerted mechanism.

An important question in studies of membrane protein insertion and folding concerns the mechanism of polypeptide chain translocation across the lipid bilayer. For example, it is unclear whether the polypeptide chain segments of polytopic membrane proteins cross the lipid bilayer individually or in a concerted fashion. This issue is especially critical for polypeptide sequences of membrane proteins that contain β-sheets or α-helices with polar residues in the membrane-spanning segments, because nonlocal intramolecular hydrogen-bonding patterns and charge interactions will critically depend on the mechanism of chain translocation. Elaborate protein translocation complexes are necessary for the translocation of secreted and the assembly of constitutive integral membrane proteins in most biological membranes. However, mechanistic details of how these complexes work and assist in the folding of polytopic integral membrane proteins are still very scarce [see Matlack et al. (*1*) for a recent review]. Especially the steps involved in releasing the newly synthesized proteins from this complex into the lipid bilayer are essentially unknown. Nevertheless and irrespective of the precise mechanism of this process, interactions of the incompletely folded polypeptide chain with the lipid bilayer will be critical at some stage of folding and will ultimately determine the native structure of integral membrane proteins.

It has been proposed that helical bundle membrane proteins fold in a two-stage process in which individual transmembrane helices fold as autonomous domains (stage I) and then pack by lateral association in the plane of the membrane (stage II) (*2*). This mechanism sensibly explains the folding of proteins with completely hydrophobic transmembrane domains but poses problems for proteins with polar side chains in the transmembrane helices such as those in ion channels. The situation becomes particularly severe for the case of

* Corresponding author. Phone: (804) 982-3578. Fax: (804) 982-1616. E-mail: lkt2e@virginia.edu.

[‡] University of Virginia Health Sciences Center.

[§] University of Groningen.

β-barrel membrane proteins in which hydrophobic and hydrophilic side chains alternate and in which a large number of backbone hydrogen bonds would have to be broken if individual β-strands spanned the membrane as autonomous folding units. Therefore, to distinguish between sequential and concerted folding mechanisms, it is of interest to separately monitor membrane insertion and translocation of the individual membrane-spanning segments of integral membrane proteins.

Until now, techniques to follow the translocation of polypeptide chains across lipid bilayers in real time and at relatively high spatial resolution have been lacking. The technique of time-resolved distance determination by fluorescence quenching (TDFQ)[1] presented in the accompanying paper (*3*) fills this gap. This technique uses covalently linked quenchers, such as bromine atoms, at different depths in the lipid bilayer. We have shown that movements of tryptophans across lipid bilayers can be monitored with high precision with this technique. The utility of TDFQ was demonstrated with wild-type outer membrane protein A (OmpA) of *Escherichia coli*. OmpA forms an eight-stranded β-barrel in the outer membrane of *E. coli* and in lipid model membranes (*4−7*). Proteinaceous facilitators of protein insertion and translocation are not known to exist in the outer membranes of Gram-negative bacteria, and OmpA is known to spontaneously fold and insert into pure lipid model membranes (*8*). Wild-type OmpA contains five tryptophans, which are all located within the β-barrel and near the polar headgroup region of the lipid bilayer (*3, 4, 7*) (see also Figure 11 for a topological model of OmpA). According to these predictions, Trp-7 is expected to reside at the periplasmic interface of the first β-hairpin, whereas Trp-15, Trp-57, Trp-102, and Trp-143 are located at the extracellular interface, one in each transmembrane β-hairpin. Therefore, by studying the translocation kinetics of individual tryptophans in single Trp mutants of OmpA by TDFQ, we can ask the question whether the individual predicted β-hairpins of OmpA translocate across the membrane sequentially or in a concerted fashion. Our results confirm a concerted mechanism for OmpA insertion and folding in lipid bilayers.

MATERIALS AND METHODS

Bacterial Strains, Phages, and Growth Media. Unless indicated otherwise, strains were grown in Luria−Bertani (LB) broth or on LB−agar supplemented with 50 μg of ampicillin/mL, 0.5% (w/v) glucose, or 1 mM isopropyl 1-thio-β-D-galactopyranoside, as required. Plasmids expressing proOmpA mutants were transformed into *E. coli* MC4100rh⁻ [F⁻, *araD139Δ(argF-lac)U169, rpsL150* (Str^r), *erlA1, flbB5301 deoC1 ptsF25, rbsR, recA*, Ox2^r] or JC6650 [*lac, proAB, rpsL, recA1, supF*(F′, *proAB⁺, lacI^q, lacZΔM14*)], which are *OmpA⁻* strains (*9*). Phages K3 (*10*) and Ox2 (*11*) have been described. They were propagated in strain JC6650 using LB broth as described (*9*).

Oligonucleotide-Directed Mutagenesis. The procedure for exchange of tryptophan residues by phenylalanine by site-

Table 1: Mismatch and PCR Primers Used for Oligonucleotide-Directed Mutagenesis

Amino Acid Substitution	Mismatch Oligonucleotides[a]
W7F	AACACCTT**C**TACACT<u>GGCGCC</u>AAACTGGG *Nar*I
W15F	CTAAACTGGGCTT**C**T**C**TCAGTACCATG *Dde*I
W57F	AAATGGGTTAC<u>GAATTC</u>TTAGGTCGTAT *Eco*RI
W102F	GTGGCATGGTATT**C**CGGGCCGACACT *Nci*I
W143F	CGCTACCCGT**C**TAGAATACCAGTTCACCAACAACATC *Xba*I
D109N	CACTAAATCCAAC<u>GTATAC</u>GGTAAAACC *Aac*I

Amino Acid Substitution	PCR Primers[a]
F7W	forward 1, 5' GATAACACCT**GG**TACACTGGTGCCAAACTG reverse 1, 5' CGCTACCCG<u>TCTAGA</u>ATACCAGTTCACCAACAACATC *Xba*I forward 2, 5' GCGCAAA<u>CCATGG</u>CAAAAAAGACAGC *Nco*I
F57W	forward 1, 5' GGGTTACGACTGG**TT**AGGTCG reverse 1, 5' CGCTACCCG<u>TCTAGA</u>ATACCAGTTCACCAACAACATC *Xba*I forward 2, 5' GCGCAAA<u>CCATGG</u>CAAAAAAGACAGC *Nco*I
F143W	forward 1, 5' CCCGTCTGGAATACCAGT**GG**ACCAACAAC reverse 1, 5' CGTCTTTCGGATCCAGGTTG forward 2, 5' AAATGGGTTAC<u>GAATT**C**</u>TTAGGTCGTAT *Eco*RI

[a] Introduced restriction sites are underlined. Mismatched nucleotides are shown in boldface.

directed mutagenesis was essentially that of Kunkel et al. (*12*). Uracil-containing single-stranded template DNA was obtained by growing the helper phage M13KO7 on *E. coli* CJ236 (*dut, ung1, thi-1, relA1, spoT1, mcrA,* [F′ cat-(= pCJ105; M13^{s}Cm^r)]) (*13*). The mismatch oligonucleotides (Eurosequence, Groningen, The Netherlands), the resulting amino acid substitutions, and the introduction of endonuclease restriction sites are shown in Table 1. The oligonucleotides were annealed to single-stranded DNA containing the *Eco*RV−*Hin*cII and *Hin*cII−*Bam*HI restriction fragments of *ompA*, which had been cloned in pBluescript-II KS(+) (Stratagene, La Jolla, CA). The complementary strand was synthesized by T4 polymerase (Boehringer Mannheim, Germany) using the mismatch oligonucleotide(s) as primer-(s). The resulting double-stranded DNA was transformed to JM109 [*recA1, endA1, gyrA96, thi⁻, hsdR17, relA1, supE44, Δ(lac-proAB),* (F′, *traD36, proAB, lacI^q M15*)] (*14*) or DH5α [*supE44, ΔlacU169 (Φ80lacZΔM15), hsdR17, recA1, endA1, gyrA96, thi-1, relA1*] (*15*). To reintroduce unique tryptophan residues, *ompA* fragments were amplified by the polymerase chain reaction (PCR), using the primers shown in Table 1. All PCR reactions were performed with *PWO* polymerase (Boehringer Mannheim, Germany) using a Biometra triothermoblock and employing the manufacturer's recommendations. The PCR products restored the wild-type genotype at the particular Trp-encoding DNA triplet. In addition, an *Nco*I site was introduced in the start codon to facilitate cloning in the expression vector pTRC99A, resulting in an additional amino acid (Ala) after the first methionine. The PCR products were cloned in pBluescript-II SK(+) or in a derivative with a *Nco*I site (pET401). All constructs were sequenced on a Vista DNA sequencer 725 (Amersham) using the automated Δtaq sequencing kit of Amersham. The mutagenized *ompA* fragments were recombined and cloned

---

[1] Abbreviations: *m,n*-DiBrPC, 1-palmitoyl-2-(*m,n*-dibromo)stearoyl-*sn*-glycero-3-phosphocholine; DOPC, 1,2-dioleoyl-*sn*-glycero-3-phosphocholine; EDTA, ethylenediaminetetraacetic acid; OmpA, outer membrane protein A; PAGE, polyacrylamide gel electrophoresis; SDS, sodium dodecyl sulfate; SUV, small unilamellar vesicle; TDFQ, time-resolved distance determination by fluorescence quenching; Trp, tryptophan, Phe, phenylalanine; wt, wild type.

in pTRC99A to obtain a Trp-less proOmpA and five proOmpA mutants containing an unique Trp (Table 1). All DNA manipulation techniques were performed essentially as described by Sambrook et al. (*16*).

Refolding Experiments and Fluorescence Spectroscopy. Recombinant OmpA was expressed in MC4100rh⁻ cells and purified as previously described (*3, 5*). Refolding experiments and time-resolved distance determinations by fluorescence quenching were carried out as described in the accompanying paper (*3*). However, due to the decreased Trp fluorescence in the single Trp OmpA mutants, we increased the concentration of mutant OmpA to 2.28 μM in all experiments. A molar lipid/protein ratio of 500 was used in all experiments. Protein concentrations were determined by the Bradford protein assay (*17*).

RESULTS

Site-Directed Mutagenesis. To study the kinetics of membrane insertion and refolding of OmpA in lipid bilayers at the level of individual topological units of the protein, we introduced unique tryptophan residues as site-specific fluorescent probes. Since the wild-type protein contains five native tryptophans, we first replaced, by site-directed mutagenesis, all tryptophans in OmpA by phenylalanines. The mutagenesis introduced, apart from the desired mutations, also a mutation at amino acid residue 109 (Asn → Asp). Although this introduction of a negative charge had no influence on the processing and translocation of proOmpA nor on its targeting to the outer membrane, this mutation was reversed to Asn (Table 1). To prevent further mutagenesis of the nucleotide triplet coding for Asn88, the codon usage in the vicinity of the triplet was changed and an *Aac*I site was introduced (Table 1). PCR mutagenesis was then used to reintroduce the unique Trp residues (Table 1). These unique tryptophans occur in positions Trp-7, Trp-15, Trp-57, Trp-102, and Trp-143, respectively. According to the topological model of OmpA (*4, 7*) (see also Figure 11), all five Trps are localized near the interfacial region of the lipid bilayer, Trp-7 on the periplasmic side and the other Trps on the extracelluar side of the outer membrane.

Folding of OmpA Mutants in Vivo. All mutant OmpAs were targeted to the outer membrane as assayed by a phage binding test. The T-even phages K3 and Ox2 use *E. coli* OmpA as a receptor and cannot infect mutants which lack this protein. The progeny of a single plaque of each phage was grown on the *ompA⁻ E. coli* strain JC6650 which was transformed with a plasmid containing either the wild-type or one of each of the mutant *ompA* genes. Clear plaques with frequencies of ∼10⁹ and ∼10⁷ pfu/mL for K3 and Ox2, respectively, appeared in all transformants harboring the single Trp mutants of OmpA (Table 2). Since K3 and Ox2 recognize different epitopes of OmpA (*18*), it can be concluded that the four Phe substitutions in each of the five single Trp mutants did not significantly alter the topology and extracellular surface structure of OmpA. Therefore, the five single Trp mutant OmpAs appear to fold *in vivo* as wt OmpA.

Tryptophan Fluorescence of Unfolded and Refolded OmpA Mutants. All OmpA mutants were expressed in the *ompA⁻ E. coli* strain MC4100rh⁻F′ and purified to homogeneity by the same procedure previously developed for wt OmpA.

Table 2: Plasmids Used and Phage Infection Efficiency of *E. coli* JC6650 Cells Expressing the Corresponding Mutant OmpAs

plasmids	description	K3 (pfu/mL)	Ox2 (pfu/mL)	source
pET185	proOmpA(ΔW)	10⁸	10⁷	this work
pET1102	proOmpA(W7)	10⁹	10⁷	this work
pET1115	proOmpA(W15)	10⁹	10⁷	this work
pET187[a]	proOmpA(W57)	10⁹	10⁷	this work
pET186	proOmpA(W102)	10⁹	10⁷	this work
pET1103	proOmpA(W143)	10⁹	10⁷	this work
pET149[a]	proOmpA	nd[b]	nd[b]	this work
pET1113	(His)₆proOmpA	10⁹	10⁷	this work
pTRC99A	Amp trc promoter	0	0	27

[a] Parental vector is pUC18. All other constructs are cloned in pTRC99A. [b] Not determined.
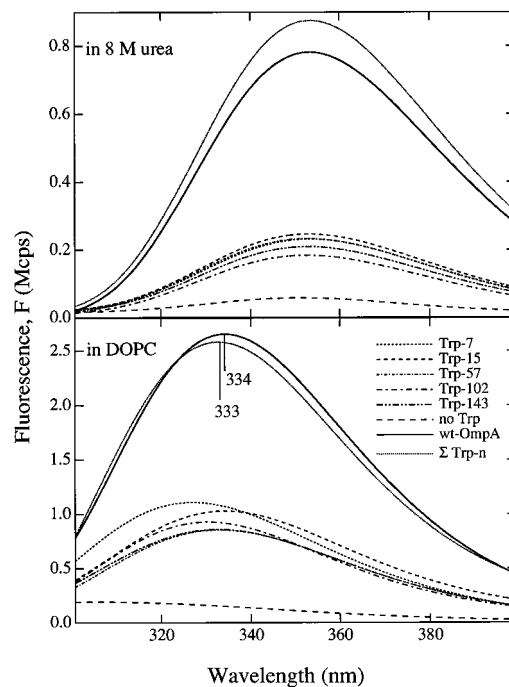

FIGURE 1: Fluorescence emission spectra of wild-type and single Trp mutant OmpAs unfolded in 8 M urea (upper panel) and refolded in vesicles of DOPC (lower panel). Also shown are the respective sums of all mutant spectra from which the tyrosine fluorescence spectrum of the Trp-less mutant OmpA has been subtracted four times (dotted line). The summed spectra are in good agreement with the corresponding spectra of wild-type OmpA at equivalent concentrations. The spectra of refolded OmpA were recorded 80 min after mixing 2.29 μM protein (1.43 μM for wt) with DOPC vesicles at a lipid/protein ratio of 500/1 at 40 °C. Spectra of unfolded OmpAs were recorded at 20 °C with 2.15 μM (1.07 μM for wt) OmpA in 10 mM glycine buffer, pH 8.5, containing 2 mM EDTA, 150 mM NaCl, and 8 M urea. Wavelength maxima were obtained by fitting spectra to a log-normal distribution.

Fluorescence spectra of unfolded and refolded wt and mutant OmpAs were recorded in 8 M urea and in DOPC vesicles, respectively (Figure 1). As expected, the urea-denatured Trp-less mutant of OmpA showed very low fluorescence in the region 300−400 nm when excited at 290 nm. The remaining background fluorescence is probably due to the 17 tyrosine residues of OmpA. In 8 M urea, all single Trp mutants and wt OmpA exhibited fluorescence emission maxima at 354 nm. The sum of all single Trp mutant spectra (each corrected by subtraction of the tyrosine background fluorescence of the Trp-less mutant) in 8 M urea is similar in shape and only about 10% more intense when compared with the
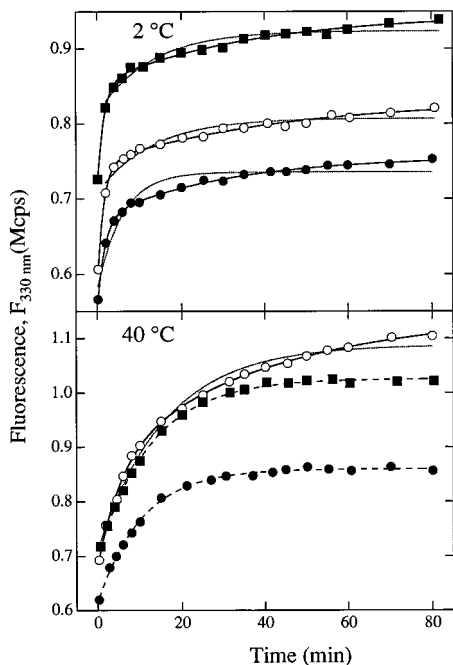
FIGURE 2: Refolding kinetics of single Trp mutant OmpAs monitored by fluorescence of Trp-7 (○), Trp-15 (■), and Trp-143 (●) at 2 °C (upper panel) and at 40 °C (lower panel). At 2 °C, all three curves follow double exponential time courses (solid lines) while single exponential fits (dotted lines) are unsatisfactory. At 40 °C, the time courses of Trp-15 and Trp-143 (as well as those of Trp-57 and Trp-102; not shown) are single exponential (dashed lines), but the kinetics of Trp-7 are better represented by a double exponential (solid line) than a single exponential fit (dotted line).

Table 3: Rate Constants of the Fluorescence Kinetics for Refolding of Single Trp Mutants in DOPC Bilayers at 2 and 40 °C

T (°C)	OmpA mutant	A_1[a]	k_1[b] (min⁻¹)	k_2 (min⁻¹)	k_3 (min⁻¹)
2	Trp-7	0.66	0.65 ± 0.04	0.025 ± 0.01	
2	Trp-15	0.53	0.56 ± 0.07	0.025 ± 0.01	
2	Trp-57	0.66	0.70 ± 0.10	0.025 ± 0.01	
2	Trp-102	0.46	0.66 ± 0.15	0.021 ± 0.01	
2	Trp-143	0.55	0.74 ± 0.06	0.034 ± 0.01	
2	wild type[c]	0.54	0.24	0.006	
40	Trp-7	0.45		0.16 ± 0.03	0.03 ± 0.01
40	Trp-15	1.0		0.08 ± 0.01	
40	Trp-57	1.0		0.11 ± 0.01	
40	Trp-102	1.0		0.08 ± 0.01	
40	Trp-143	1.0		0.10 ± 0.01	
40	wild type[c]	1.0		0.12	

[a] Relative amplitudes of faster process. [b] Rate constants for refolding. [c] Data from ref 8.

corresponding spectrum of wt OmpA, showing that the fluorescence of the mutants is approximately additive. Refolded into DOPC bilayers, the fluorescence intensity of the Trp-less mutant was still low, but shifted to 306 nm. All single Trp mutants showed blue shifts of the fluorescence emission maxima by at least 20 nm. The maxima were at 327 nm (Trp-7), 334 nm (Trp-15), 333 nm (Trp-57 and Trp-143), and 330 nm (Trp-102). Summation (after correction for fluorescence of the Trp-less mutant) of all mutant spectra in DOPC resulted in an emission maximum at 333 nm, very close to that of wild-type protein (334 nm), again showing excellent additivity even in the folded structure of OmpA.

Refolding of OmpA Mutants in Vitro. All five mutants of OmpA spontaneously refolded into DOPC vesicles where they formed a trypsin-protected 24 kDa fragment just as the wt protein (8). The refolded mutant proteins also exhibited ion channel activities in planar lipid bilayers similar to that of wt OmpA (Arora and Tamm, in preparation). In Figure 2, we show the time courses of the refolding reactions of the single Trp mutants Trp-7, Trp-15, and Trp-143 into lipid bilayers as monitored by fluorescence spectroscopy at 2 and 40 °C. At 2 °C, refolding proceeds only to membrane-bound intermediate I_{M2}, and the fluorescence kinetics are well described by double exponential fits as previously observed for the wt protein (8). In contrast, at 40 °C, the fluorescence kinetics of Trp-15 and Trp-143 are single exponential like those of the wt protein. The kinetics of two other single Trp mutants, Trp-57 and Trp-102, were similar to those of Trp-15 and Trp-143 (data not shown). The only minor difference from wt OmpA was observed with Trp-7, which was better fit by a double exponential function even at 40 °C. The rate constants of the kinetic analyses of all mutants in the absence

of quenchers are summarized and compared to those of wt OmpA in Table 3. At 2 °C, rate constants observed for the two kinetic steps were very similar for all five single Trp mutants. The first step was more than an order of magnitude faster than the second step, consistent with earlier results on wt-OmpA (8). In the first step, fluorescence sharply increased within the first 2 min from relatively low emission in 8 M urea (see Figure 1, upper panel), reflecting adsorption to the bilayer surface (intermediate I_{M1}). In the subsequent step, all mutants showed a further, but quantitatively smaller, increase in fluorescence intensity leading to intermediate I_{M2}. In contrast, at 40 °C, differences were found between Trp-7 and all other mutants. While Trp-15, Trp-57, Trp-102, and Trp-143 showed single exponential fluorescence kinetics with rate constants between 0.08 and 0.11 min⁻¹, two steps were distinguished for Trp-7 with rate constants of 0.16 and 0.03 (averaged from three experiments). These rate constants were both smaller than those observed at 2 °C. However, the faster rate constants observed for all mutants at 2 °C are not resolved at 40 °C. We therefore assign the small rate constant observed for Trp-7 at 40 °C to a third, slow step of refolding, which is only observable with this mutant.

Fluorescence Quenching of Single Trp Mutants at 40 °C. To determine the final location of each Trp residue after complete refolding of OmpA, we first measured the kinetics of membrane incorporation of each of the five single Trp mutants at 40 °C in the presence of four different brominated lipids, which served as positional quenchers of Trp fluorescence (Figure 3). Only the last steps of OmpA refolding and insertion are observed at this temperature (3, 8). The four three-dimensional graphs of Figure 3 show the evolution of fluorescence intensity as a function of time and position of the quenching bromine atoms in the course of refolding of the single Trp mutants Trp-7, Trp-15, Trp-57, and Trp-143 at 40 °C. For each mutant, these time courses were monitored with five different samples, four of which contained 30 mol % of 4,5-, 6,7-, 9,10-, and 11,12-DiBrPC, respectively, in DOPC and a fifth reference sample which consisted of DOPC only. The distances of the quenching bromine atoms from the bilayer center (19) are given on the x-axis of each graph, and the reference without quencher is plotted on the far right of each 3-D graph. Similar graphs were also obtained for the Trp-102 mutant (data not shown). We first note that Trp-7 is more effectively quenched than Trp-15, Trp-57, and Trp-143 (and Trp-102) by all quenchers at long times. The
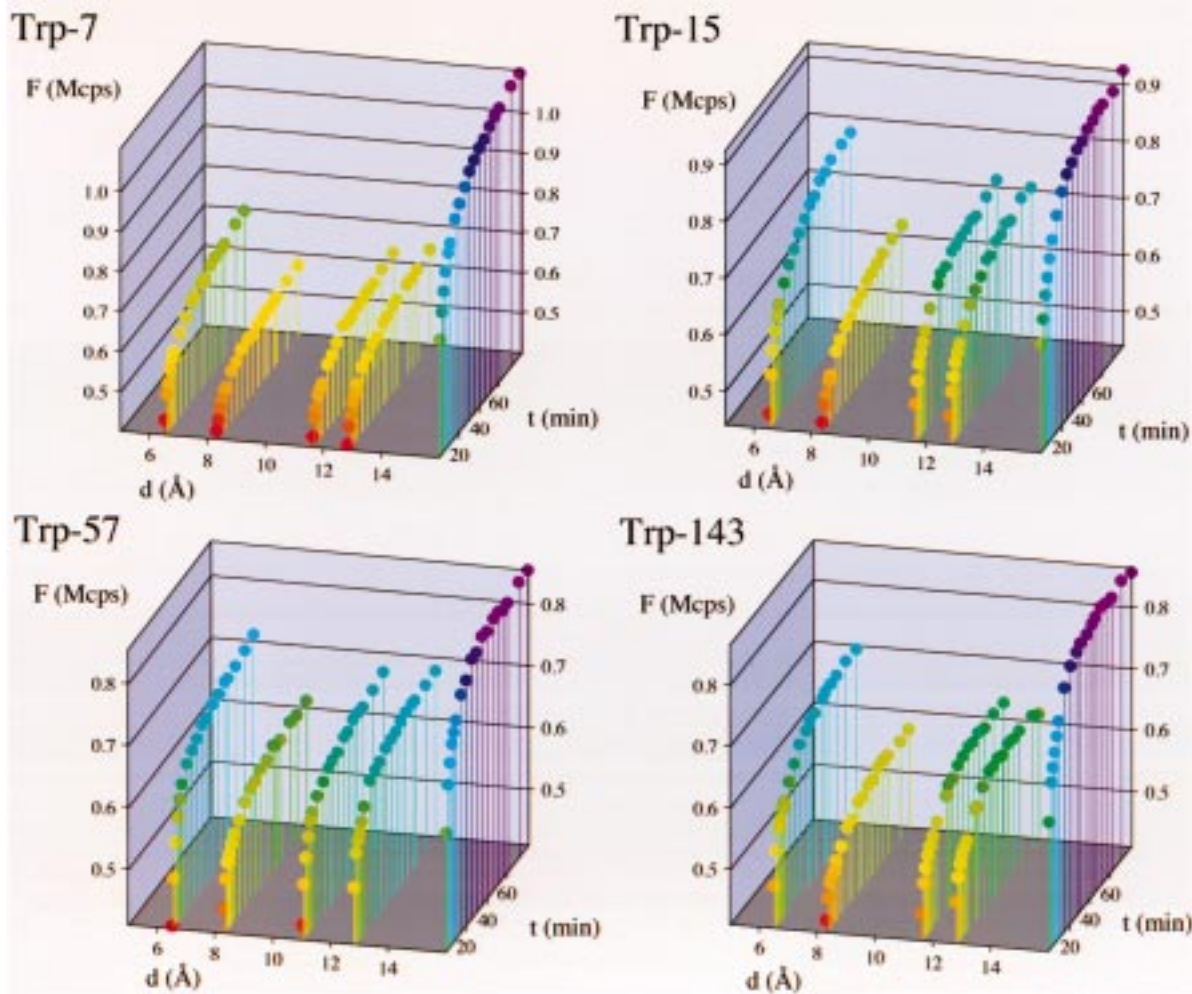
FIGURE 3: Trp fluorescence intensities of four single Trp mutants of OmpA (Trp-7, Trp-15, Trp-57, and Trp-143) at 330 nm as a function of time and bromine distance from the bilayer center measured at 40 °C. Lipid vesicles composed of DOPC and 30 mol % of either 11,12-, 9,10-, 6,7-, or 4,5-DiBrPC, with average quencher distances from the bilayer center of 6.5, 8.3, 11.0, and 12.8 Å, respectively, were used (*3*). The reference curves on the right of each distance axis were measured with pure DOPC vesicles. Equivalent plots of the fifth single Trp mutant (Trp-102) closely resemble that of Trp-15 (data not shown).

quenching efficiency is usually assessed by normalizing the quenched fluorescence, $F(d_Q)$, to the reference fluorescence in the absence of quencher, F_0. After averaging $F(d_Q)/F_0$ at 80 min over all four brominated lipid quenchers, we found $F(d_Q)/F_0$ values of 0.59, 0.75, 0.76, 0.82, and 0.73 for Trp-7, Trp-15, Trp-57, Trp-102, and Trp-143, respectively. Second, the 9,10-DiBrPC quencher was the most effective of all quenchers after completion of membrane incorporation and folding for all five single Trp mutants. The shallower quenchers 6,7- and 4,5-DiBrPC were the next effective, and the deep quencher 11,12-DiBrPC was the least effective quencher. This result already indicates that all five Trp positions of refolded OmpA will be around 10 Å from the bilayer center. However, the order of quenching at earlier times of refolding is not necessarily the same (see for example, the first data points of Trp-7 in Figure 3), as can be further verified by performing similar experiments at lower temperatures. Therefore, we measured time-resolved fluorescence quenching profiles for each of the five mutants at temperatures between 2 and 40 °C.

Time-Resolved Fluorescence Quenching Profiles of Trp-7. To determine Trp positions in the lipid bilayer at different stages of refolding, we performed time-resolved fluorescence quenching experiments at various temperatures between 2

and 40 °C. The data were analyzed by first plotting fluorescence quenching profiles $F(d_Q)/F_0$ at each time and temperature (*3*). To determine the distance d_{Trp} of the fluorophore (Trp) from the bilayer center, the quenching profiles were then fitted to eq 1 as described (*3, 20*). F_0 and

$$\frac{F(d_Q)}{F_0} = \exp\left\{-\frac{S}{\sigma\sqrt{2\pi}}\exp\left\{-\frac{1}{2}\left(\frac{d_Q - d_{Trp}}{\sigma}\right)^2\right\}\right\} \quad (1)$$

$F(d_Q)$ in eq 1 are the fluorescence intensities in the absence and in the presence of a particular m,n-DiBrPC quencher and d_Q is the distance of the quencher from the lipid bilayer center. The dispersion, σ, is a function of the sizes of the fluorophore and quencher and of thermal fluctuations between the two, and S is a function of the quenching efficiency and quencher concentration in the membrane. Figure 4 shows $F(d_Q)/F_0$ plots of Trp-7 at different times at 2 °C (upper panels) and at 40 °C (lower panels). 11,12-DiBrPC, which is located at 6.5 Å from the bilayer center (*19*), was the least effective quencher of Trp-7 under all conditions. At both temperatures, 4,5-DiBrPC ($d_Q = 12.8$ Å) was the most effective quencher 20 s after initiation of the folding reaction. In the very beginning of the refolding process quenching profiles were shallow and indicated an
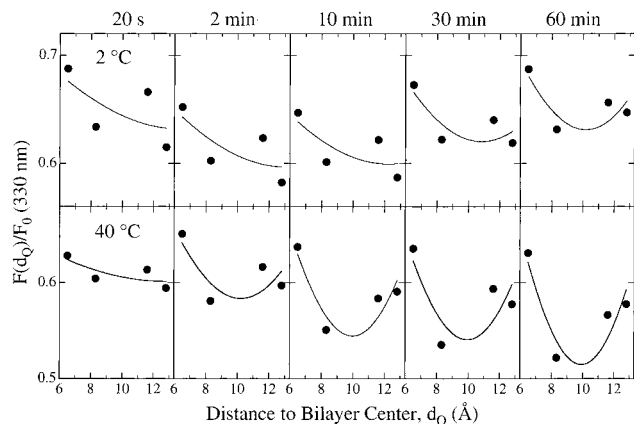
FIGURE 4: Fluorescence quenching profiles of Trp-7 OmpA at 2 °C (upper panels) and at 40 °C (lower panels) after 20 s and 2, 10, 30, and 60 min. The profiles were generated by plotting the fluorescence ratios $F(d_Q)/F_0$ as a function of quencher distance from the bilayer center. The solid lines represent best fits of the data to eq 1. The minima of the fits indicate the average positions of the Trp residues in each case.
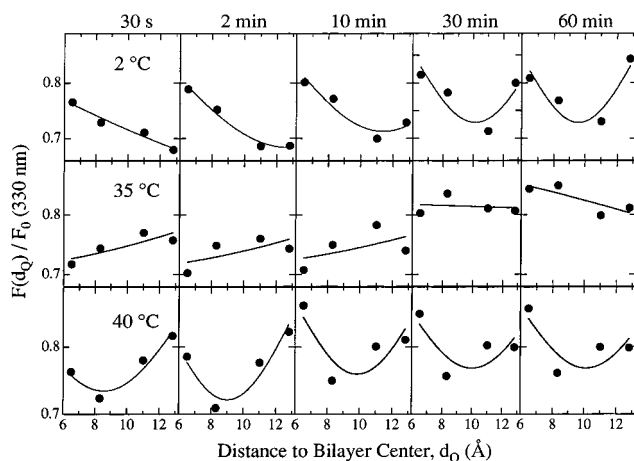

FIGURE 5: Fluorescence quenching profiles of Trp-102 OmpA as a function of time after initiation of OmpA refolding into lipid bilayers at 2, 35, and 40 °C. Profiles were generated and fits were performed as described for Figure 4.

(average) location of Trp-7 close to the bilayer surface. After 30−60 min at 2 °C or after 2 min at 40 °C, the width of the profile, σ, became more narrow, and the Trp-7 location was found at 10 Å from the center of the lipid bilayer.

Time-Resolved Fluorescence Quenching Profiles of Trp-102. Similar fluorescence quenching profiles are shown in Figure 5 for the Trp-102 mutant of OmpA at 2, 35, and 40 °C. At 2 °C, Trp-102 was most strongly quenched by 4,5-DiBrPC 30 s after initiation of the refolding reaction. Less quenching was observed with decreasing distance of the quenchers from the bilayer center. At later times, the fluorescence quenching profiles indicated that Trp-102 had moved deeper into the bilayer to a distance of about 10 Å. The initial quenching profiles, observed within the first 2 min, were very different at 40 °C when compared to those at 2 °C. At 40 °C, Trp-102 fluorescence was most strongly quenched deep in the bilayer, whereas the quenchers located closer to the membrane surface were less effective. At later times, 11,12-DiBrPC and 9,10-DiBrPC became less effective quenchers, and the quenching efficiency of 4,5-DiBrPC increased. Intermediate situations were observed at intermediate temperatures. For example, at 35 °C (middle panels of
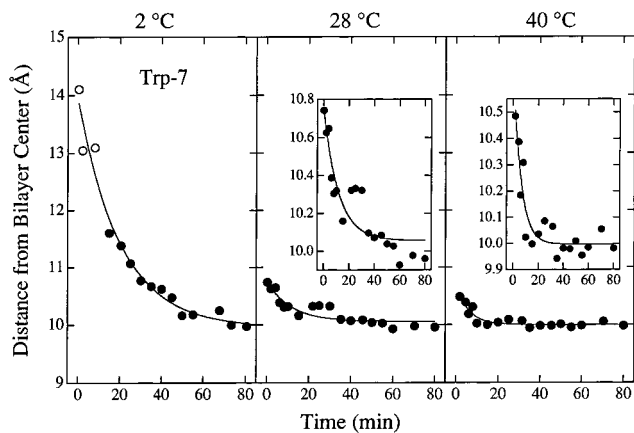

FIGURE 6: Time courses of the movement of Trp-7 toward the bilayer center at 2, 28, and 40 °C. Distances were obtained from curve fits of the fluorescence quenching profiles as shown in Figure 4. The insets at 28 and 40 °C show the data on expanded distance scales. Data points represented by closed circles were the fitted quenching profile minima, and open circles denote extrapolated distances from the observed quenching profiles. The solid lines are fits of the data to single or double exponential functions (see text).

Figure 5), a gradual change from a deep to a surface location was observed. Moreover, the profiles were very broad, indicating a large dispersion, σ, of the Trp distribution across the lipid bilayer. Similar effects were seen for wt OmpA at intermediate temperatures (*3*). Plots similar to those of Figure 5 were also obtained for the Trp-15, Trp-57, and Trp-143 mutants (data not shown).

Time-Resolved Distance Determination of Trp-7. In Figure 6, the time courses of the (average) Trp-7 locations along the membrane normal were derived from 18 different fluorescence quenching profiles obtained within 80 min at each temperature (2, 28, and 40 °C, respectively). At all three temperatures, Trp-7 started from a farther distance and approached a distance of 10 Å from the bilayer center. The first observable distances at 20 s after mixing were 14.2, 10.8, and 10.5 Å at 2, 28, and 40 °C, respectively. The distance decrease was faster at the higher temperatures and single exponential fits gave translocation rate constants of 0.05, 0.085, and 0.16 min^{-1} at 2, 28, and 40 °C, respectively, for the movement of Trp-7 into the bilayer. The decrease of the Trp distance from the bilayer center to 10 Å at 40 °C was confirmed in additional experiments with samples consisting of 100% brominated PCs instead of the 30% which were typically used in our experiments (data not shown). The fact that Trp-7 was never found closer than ~10 Å from the bilayer center indicates that this Trp does *not* translocate across the lipid bilayer but remains on the cis side of the membrane in the course of the entire folding reaction.

It should be noted that the rates of Trp movement into and/or across the lipid bilayer, which were calculated from the data of Figure 6 (and all subsequent similar figures), are different from the rates of Trp binding and insertion into the lipid bilayer, which were determined by changes in Trp fluorescence, e.g., as shown in Figures 2 and 3. The latter are true chemical rate constants and monitor changes between two or more chemically distinct states. However, the translocation rates obtained from TDFQ reflect velocities (distance/time) of Trp movement projected onto the normal of the lipid bilayer which, however, are dampened and reach zero when the final equilibrium state is approached (see also ref *3*).
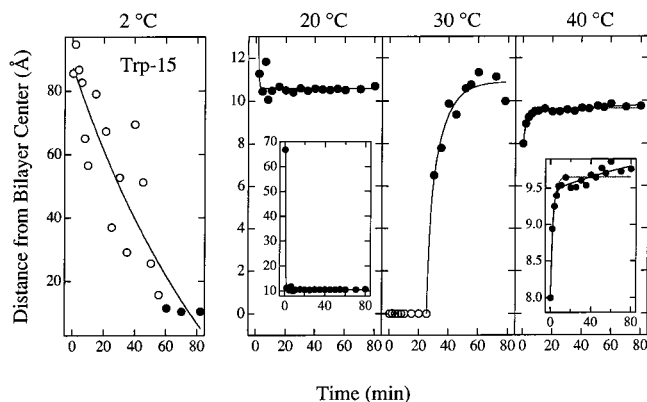
FIGURE 7: Time courses of the movement of Trp-15 toward the bilayer center at 2 and 20 °C and from the bilayer center at 30 and 40 °C. At 2 °C, Trp-15 distances from the bilayer center were large and could only be obtained by extrapolation (open circles). The solid lines are fits of the data to single or double exponential functions (see text).

FIGURE 9: Time courses of the movement of Trp-102 toward the bilayer center at 2 and 22.5 °C and from the bilayer center at 40 °C. The inset at 40 °C shows the same data on an expanded distance scale. The solid lines are fits of the data to single or double exponential functions (see text).
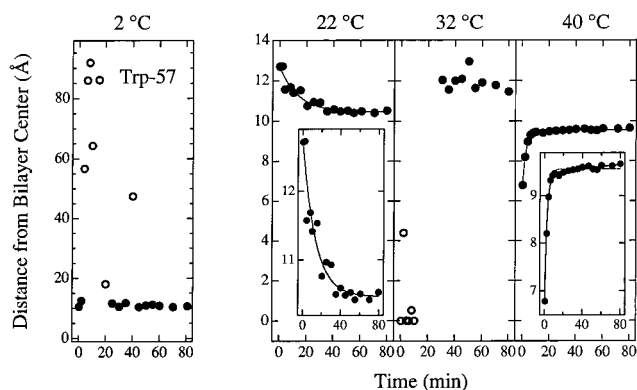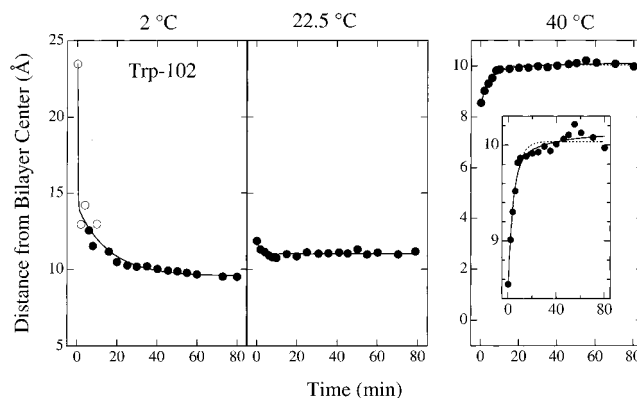

FIGURE 8: Time courses of the movement of Trp-57 toward the bilayer center at 2 and 22 °C and from the bilayer center at 32 and 40 °C. Insets with an expanded distance scale are shown for temperatures 22 and 40 °C. Where possible, the data were fit to single or double exponential functions, represented by solid lines (see text).
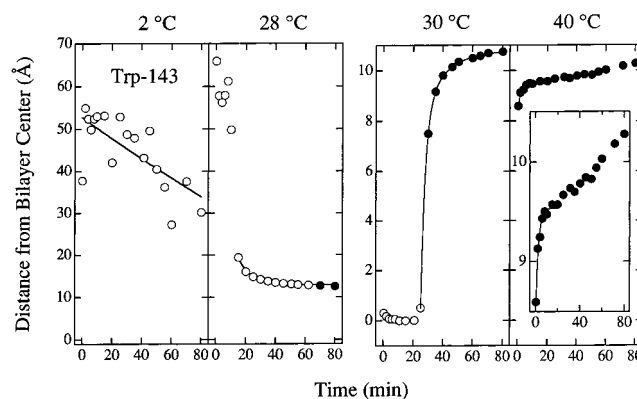

FIGURE 10: Time courses of the movement of Trp-143 toward the bilayer center at 2 and 28 °C and from the bilayer center at 30 and 40 °C. At 2 °C, the distances of Trp-143 could only be obtained by extrapolation (open circles). The solid lines are fits of the data to single or double exponential functions (see text).

Time-Resolved Distance Determination of Trp-15. Figure 7 shows the distances of Trp-15 from the bilayer center as functions of time at 2, 20, 30, and 40 °C. At 2 °C, the distance of Trp-15 was found to decrease to 10 Å within 60 min. At 20 °C, Trp-15 approached a 10−12 Å distance within a minute but did not penetrate the lipid bilayer any further. Trp-15 was also observed to approach this distance at 25 and 28 °C (data not shown). At 30 °C, Trp-15 was found initially in the center of the lipid bilayer and remained in this location for the first 25 min. Subsequently, Trp-15 moved from the center to 10−11 Å in a biphasic process with translocation rate constants of 0.58 and 0.10 min^{-1}.

Time-Resolved Distance Determination of Trp-57. Distances of Trp-57 from the bilayer center as a function of time are shown in Figure 8 at 2, 22, 32, and 40 °C. At 2 and 22 °C, this Trp residue approached a distance of 10−12 Å from the bilayer center within ∼40 min. Extrapolations (indicated by open circles) of fluorescence quenching profiles at 2 °C indicate that this Trp may be found at larger distances from the bilayer center within the first few minutes of the folding reaction. The same 10 Å distance was also found in additional refolding experiments at 25 °C. The quenching profiles obtained at 32 °C localized Trp-57 close to the lipid bilayer center during the first 15 min, but this Trp moved to

a 12 Å distance at later times, similar to Trp-15. At 40 °C, the distance of Trp-57 increased from ∼6.8 to 9.5 Å from the lipid bilayer center within a few minutes. A double exponential fit of the outward movement of Trp-57 gave translocation rate constants of 0.46 and 0.005 min^{-1} for this process.

Time-Resolved Distance Determination of Trp-102. Time-resolved distances of Trp-102 from the bilayer center are shown in Figure 9. At 2 °C, the distance of Trp-102 to the bilayer center decreased to 10 Å within 20 min. A fit to a single exponential function yielded a rate constant of 0.063 min^{-1} for this process. Approximately the same distance (11 Å) was approached from the outside at 22.5 °C. At 40 °C, the distance of Trp-102 to the bilayer center increased with time from 8.5 to 10 Å. A double exponential fit of these time courses yielded translocation rate constants of 0.26 and 0.03 min^{-1}.

Time-Resolved Distance Determination of Trp-143. Figure 10 shows the time courses of the distance changes of Trp-143 from the bilayer center at 2, 28, 30, and 40 °C. At 2 °C, distances calculated from the fluorescence quenching profiles using eq 1 were large and could only be extrapolated. The estimated distances of Trp-143 were greater than 25 Å at all times at 2 °C. Therefore, Trp-143 behaved differently from Trp-7, Trp-57, and Trp-102, which were found to approach a distance of ∼10 Å from the lipid bilayer center within the

Table 4: Rate Constants of Translocation at 40 °C and Critical Temperatures for Center Crossing of Individual Trps of OmpA in DOPC Bilayers

mutant	direction[a]	$A_{t,1}$[b]	$k_{t,1}$[c] (min^{-1})	$k_{t,2}$ (min^{-1})	T_{cross}[d]
Trp-7	in	1.0	0.16		
Trp-15	out	0.69	0.55 ± 0.09	0.008 ± 0.02	30
Trp-57	out	0.84	0.46 ± 0.02	0.005 ± 0.02	32
Trp-102	out	0.82	0.26 ± 0.08	0.03 ± 0.06	35
Trp-143	out	1.0	0.43 ± 0.09		30
wt[e]	out	0.0		0.09 ± 0.01	28

[a] Sign of amplitudes: in, toward bilayer center; out, from bilayer center. [b] Relative amplitudes of faster process. [c] Translocation rate constants. [d] Critical temperature at which Trps were observed to cross the bilayer center. [e] Data from ref *3*.

first 20 min at 2 °C. Trp-15 was intermediate in this respect, because it approached 10 Å at 2 °C, but only after 60 min. At 28 °C, the distance of Trp-143 decreased from a large (extrapolated) distance to about 12 Å within the first 20 min. In contrast, at 30 °C, Trp-143 was found close to the center of the lipid bilayer for about 20 min but then moved out to 11 Å from the center. Translocation rate constants of 0.3 and 0.06 min^{-1} were determined using a double exponential fit to these data. At 40 °C, the distance of Trp-143 increased from 8.5 to 10.2 Å from the center.

Comparison of Translocation Rate Constants of Individual Tryptophans during Folding of OmpA into Lipid Bilayers. The translocation rate constants obtained from the fits of the distance time courses at 40 °C (shown in Figures 6–10) are summarized in Table 4 for all individual Trps of OmpA. The rates obtained for the faster component representing translocation of the Trps from a location near the bilayer center to about 9.5–9.8 Å from the center are very similar for Trp-15, Trp-57, Trp-102, and Trp-143, i.e., 0.3–0.5 min^{-1}. The translocation rate obtained for the inward movement of Trp-7 at this temperature is smaller. For wt OmpA, only the slower process was resolved at 40 °C. The critical temperature for the transition from intermediate I_{M3}, in which the Trps are on average located close to the center of the lipid bilayer, was found at 28 °C for wt OmpA and at 30–35 °C for the single Trp mutant OmpAs.

DISCUSSION

We have studied the translocation of individual Trp residues of the β-barrel membrane protein OmpA across the lipid bilayer during insertion and folding into pure lipid model membranes. This was accomplished by applying a new technique, time-resolved distance determination by fluorescence quenching, TDFQ (*3*), in refolding experiments with single Trp mutants of OmpA. Since four of our mutants have the single Trps located each on a different outer loop of the four predicted β-hairpins, we had the opportunity to resolve the membrane insertion process separately for each of the four topological units of the protein. The most striking result of this study is that the four β-hairpins cross DOPC bilayers nearly synchronously. We found previously that OmpA can fully insert and cross the lipid bilayer only at temperatures greater than about 28 °C (*3*). This same conclusion is reached when the crossing of individual β-hairpins is resolved: Trp-15, Trp-57, Trp-102, and Trp-143 all require activation above 30 °C to move their respective Trps across the lipid bilayer. In addition, at 40

°C, where translocation is easily achieved, the rates of Trp translocation of all four mutants are very similar. These results provide strong evidence for a concerted mechanism in which the β-barrel forms before, or more likely, during the simultaneous translocation of all four β-hairpins across the lipid bilayer. We consider formation of the β-barrel before membrane insertion unlikely because the compact 30 kDa form is only observed at the latest stages of folding (*8*) and because folding of OmpA in detergent required micelles and did not occur in monomeric detergent solutions (*21*).

There are several reasons to believe that our *in vitro* folding studies are also relevant to the insertion mechanism of OmpA *in vivo*. It has been argued that lipopolysaccharides (LPS) may be important for the insertion of proteins into the outer membrane of Gram-negative bacteria (*22*). However, LPS is only present in the outer monolayer of the outer membrane and therefore is unlikely to assist in the early folding steps *in vivo*. However, this does not exclude a role for LPS in the late membrane translocation and final folding steps of outer membrane proteins. Translocator proteins which assist polypeptide translocation of outer membrane proteins are not known to exist in this membrane. However, a periplasmic protein (Skp) with a postulated chaperone function has recently been discovered (*23*), and it will be interesting to investigate its role in the folding of OmpA. Although it is likely that Skp (or other yet to be discovered periplasmic chaperonins) will accelerate the overall folding process of outer membrane proteins, we expect that these proteins will not directly affect the mechanistic details of folding in the membrane after the protein is safely delivered to the membrane surface.

To support our conclusion of a concerted membrane insertion and folding mechanism, it is important to show that the relatively conservative four-site mutations did not affect the folding behavior of OmpA. Several arguments provide rather strong evidence for this contention. First, all single Trp mutants appear to have properly folded *in vivo* because two different phage epitopes were retained. Second, all mutants incorporated into DOPC bilayers with approximately the same kinetics as did wild-type OmpA. Third, the summed fluorescence spectra of the refolded mutants in DOPC were almost completely superimposable with the fluorescence spectrum of refolded wild-type OmpA, i.e., a result which is consistent with nearly identical tertiary structures of all proteins. Forth, all mutants formed the 30 kDa form and the characteristic 24 kDa membrane-protected trypsin fragment upon refolding into DOPC bilayers as does wt OmpA. And fifth, similar single-channel properties were observed in planar lipid bilayer experiments for wt and the mutant OmpAs (Arora and Tamm, in preparation).

Our result that all four β-hairpins of OmpA insert and translocate across the membrane by a synchronous concerted mechanism is quite remarkable and differs from a popular tenet for the folding mechanism of helical bundle proteins. Mainly on the basis of theoretical arguments, Popot and Engelman (*2*) proposed a two-stage model for the folding of such proteins which posits that the transmembrane helices each form independent transmembrane folding units (stage I) which then assemble laterally to form the native three-dimensional structure (stage II). Experiments with fragments of bacteriorhodopsin partially supported this model (*24, 25*). The folding of a β-barrel protein is fundamentally different

from the folding of α-helical bundle proteins. Both structures are stabilized in the membrane by the formation of intramolecular hydrogen bonds. However, hydrogen bonds are formed within each helix of the bundle in helical membrane proteins, whereas hydrogen bonds are formed between neighboring strands in β-barrel proteins. Therefore, it is not surprising that the β-barrel appears to form upon insertion into the hydrophobic part of the bilayer, which would result in the observed synchronous translocation behavior of the four translocated tryptophans. By extrapolation, one might expect that helical bundle proteins which contain many internal polar side chains (e.g., ion channels) would also insert and fold by a synchronous (or perhaps hybrid) mechanism rather than by a pure two-stage mechanism.

The present study with single Trp mutants reveals the real power of the TDFQ technique to study membrane protein folding. Rather than monitoring global properties as was the case when we studied the five Trp wild-type protein by this technique (3), we can now assign the measured movements to specific regions in the sequence of OmpA. An interesting observation is that the quenching profiles observed with the mutants are as broad as those observed with the wild-type protein. This means that the observed widths of the distribution of Trp residues in the wt protein are not necessarily due to different trans bilayer dispositions of the five Trps at different stages of folding but rather represent broad distributions of each of the individual Trps in this process or are dominated by broad distributions of the bromine atoms in site-specifically labeled liquid-crystalline lipid bilayers.

Despite the many common properties that Trp-15, Trp-57, Trp-102, and Trp-143 share with equivalent measurements on the wt protein, there are some more subtle differences that can be resolved with the single Trp mutants. At low temperatures, where intermediates I_{M1} and I_{M2} are formed, Trp-102 and Trp-57 reach the 10 Å location on the cis monolayer (I_{M2}) more quickly than Trp-15 and particularly Trp-143. It appears, therefore, that the two central β-hairpins immerse themselves into the membrane before the two peripheral β-hairpins in the sequence of OmpA. Similarly, Trp-143 shows a protracted final folding phase at 40 °C which is not observed in any of the other single Trp positions. While these differences could very well reflect true differences in the folding of individual segments of the protein, we cannot exclude the possibility that subtle changes in folding are also induced by the four Phe replacements which were introduced in different positions to generate the single Trp mutants. We think that especially the small changes in the critical translocation temperatures (28−35 °C) could be caused by the mutagenesis.

Trp-7 behaves differently from the other Trps in OmpA in many respects. First, it exhibited a larger shift in the fluorescence emission maximum (327 nm) than other mutants (typically 333−334 nm). Second, the fluorescence kinetics of Trp-7 at 40 °C are double exponential with a second, much slower phase, which is absent when measured with the other mutants (Figure 2, Table 3). Third, the fluorescence quenching profiles of Trp-7 as a function of time at 2 and 40 °C (Figure 4) show that the shallower quenchers are more effective than the deep quenchers in the first few minutes of refolding. The other Trps are already deeper at this stage of refolding. And, most importantly, TDFQ analysis shows that there are no conditions under which Trp-7 is found in the

center of the lipid bilayer (Figure 6). Instead, the distance *decreases* to a final location of 10 Å from the center *at all temperatures*. The crystal structure of OmpA, which was obtained in detergent (7) (see also Figure 11), shows that Trp-7 is in the periplasmic leaflet of the outer membrane of *E. coli*, which corresponds to the outer leaflet in our vesicular in vitro refolding system. The result that all Trps but Trp-7 translocate across the bilayer supports the same general topological model in lipid bilayers.

Since Trp-7 and Trp-15 are separated only by seven residues from each other and since they are on the same predicted β-strand, some interesting conclusions can be reached about the folding of this segment. The TDFQ results indicate that this segment is initially, i.e., in the intermediate I_{M2}, oriented mostly parallel to the membrane surface. In intermediate I_{M3}, where Trp-7 still is located 10 Å from the center, but where the other Trps are already in the bilayer center, the segment between residues 7 and 15 has to be tilted relative to the membrane surface, adopting an increasingly more perpendicular orientation of this β-strand. In the last step, leading to the fully folded state, N, this first β-strand will orient even more steeply into the membrane to satisfy the requirement of simultaneously locating Trp-7 at 10 Å on the cis side and Trp-15 at 10 Å on the trans side of the lipid bilayer. The measured trans bilayer distances are in good agreement with the 45° tilt of the β-strands in the crystal structure of OmpA (7). Eight residues of a standard β-strand are expected to span a distance of about 28 Å, but with a tilt of 45° project onto 20 Å on the bilayer normal. This distance between Trp-7 and Trp-15 in completely folded OmpA, which we measured before the crystal structure was known, is in excellent agreement with the structure that was published after submission of this paper. Although not directly monitored with additional probes, a similar sequence of events will presumably occur with the other seven transmembrane segments. This is illustrated schematically in the folding model of OmpA which is presented in Figure 11.

Figure 11 summarizes what is currently known about the last steps of folding of OmpA in a lipid bilayer (for the earlier steps, see also Figure 9 of ref 3). In this concerted folding and insertion model all four β-hairpins of OmpA assemble into a β-barrel and penetrate the lipid bilayer at the same time. According to the model, most β-structure (but not yet in the form of a β-barrel) forms at the membrane surface directly after adsorption, as was previously shown with DMPC bilayers in the gel phase by polarized ATR-FTIR (6) and CD spectroscopy (5). We view this intermediate, I_{M1}, as a series of connected, but independently folded β-hairpins, arranged in a starlike fashion like the ribs in an umbrella. In a next stage, in intermediate I_{M2}, the Trps and the hairpins of which they are part penetrate deeper into the membrane, i.e., to a location about 10 Å from the bilayer center. The two central hairpins (numbers 2 and 3) reach this location a little faster than the two peripheral hairpins (numbers 1 and 4). This intermediate may be called a "molten disk" intermediate, in analogy to the "molten globule" which is frequently observed as a folding intermediate in globular proteins. The Trps on the four outer loops of the four hairpins subsequently move to an average location to the center of the bilayer. However, their distribution across the lipid bilayer is very broad at this stage, which leads us to conclude that the I_{M3} intermediate may be best viewed as a molten globule
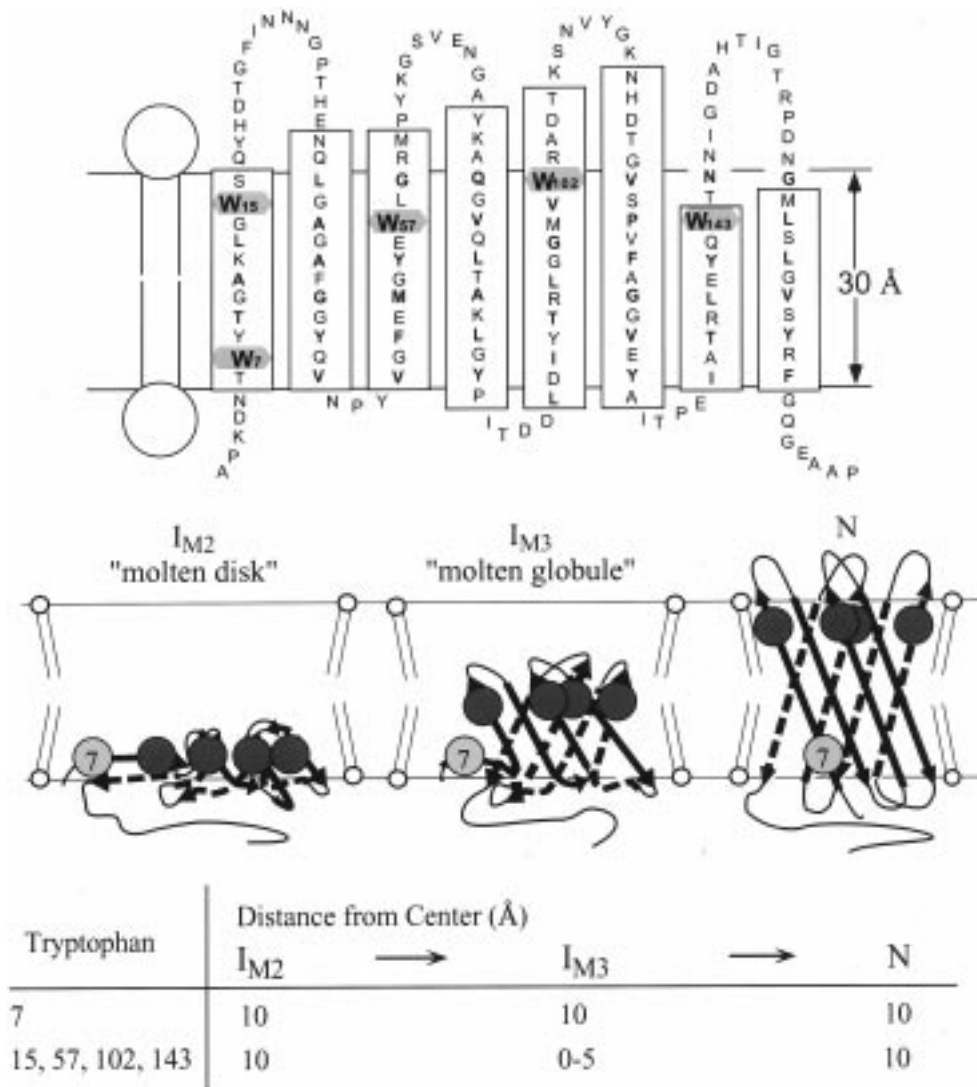
FIGURE 11: Topological model (adapted from refs *4* and *7*) and scheme for the concerted folding and insertion mechanism of OmpA. The β-strands (boxed) are on average ~45° inclined from the membrane normal (*6, 7*). Hydrophobic residues believed to be in contact with the lipid bilayer are shown in boldface. The folding model shows the nearly synchronous insertion and translocation of Trp-15, Trp-57, Trp-102, and Trp-143 across the lipid bilayer. After adsorption to the membrane surface (intermediate I_{M1}, not shown), a "molten disk" intermediate (I_{M2}) forms with all Trps at 10 Å in the cis monolayer, followed by an "inside-out molten globule" intermediate (I_{M3}) with Trps at an average location in the bilayer center and finally by the native state with the four Trps translocated to a position at 10 Å in the trans monolayer. Trp-7 stays at 10 Å in the cis monolayer throughout these late stages of folding.

analogue for membrane proteins, perhaps with some, but not all, of the β-barrel inter-hairpin hydrogen bonds formed at this stage (*3*). Relative to the normal molten globules of soluble proteins, this presumably would be an "inside-out" molten globule with the hydrophilic residues buried within the protein and the hydrophobic residues exposed to the lipid bilayer. Trp-7 remains on the cis side of the bilayer in this intermediate. Finally, to form the native folded β-barrel, the four hairpins translocate completely and position their respective outer loop Trps at about 10 Å from the bilayer center. Stable hydrogen bonding is expected to take place only at this last stage of folding, which is consistent with the late appearance of the SDS-resistant compact 30 kDa form of OmpA (*8*).

CONCLUSIONS

By applying TDFQ to study the folding of single Trp mutants of OmpA in lipid bilayers, we have observed a synchronous translocation of all four β-hairpins and a concerted folding mechnism of OmpA in lipid bilayer membranes. On the basis of these and previous data on the folding of OmpA in lipid bilayers, we have proposed a detailed multistage concerted folding model for this β-barrel protein (Figure 11; see also Figure 9 in ref *3*). Although helical bundle membrane proteins, such as seven-helix receptors or ion channels, may fold differently, some elements may be common. For example, secondary structures may rapidly form at the membrane surface (*26*) and move across the bilayer as helical hairpins either with or without the help of translocator proteins. The degree and nature of assistance by such accessory proteins will likely depend on the hydrophilic/hydrophobic balance on the surface of the translocated structural units. No such accessory proteins are known to exist in the outer membranes of Gram-negative bacteria. This may be one reason why these latter proteins have evolved as β-barrel proteins, which can insert into membranes by a self-assisted mechanism as has been shown in this work.

Kleinschmidt et al.

REFERENCES

1. Matlack, K. E. S., Mothes, W., and Rapoport, T. A. (1998) *Cell 92*, 381−390.
2. Popot, J. L., and Engelman, D. M. (1990) *Biochemistry 29*, 4031−4037.
3. Kleinschmidt, J. H., and Tamm, L. K. (1999) *Biochemistry 38*, 4996−5005.
4. Vogel, H., and Jähnig, F. (1986) *J. Mol. Biol. 190*, 191−199.
5. Surrey, T., and Jähnig, F. (1992) *Proc. Natl. Acad. Sci. U.S.A. 89*, 7457−7461.
6. Rodionova, N. A., Tatulian, S. A., Surrey, T., Jähnig, F., and Tamm, L. K. (1995) *Biochemistry 34*, 1921−1929.
7. Pautsch, A., and Schulz, G. E. (1998) *Nat. Struct. Biol. 5*, 1013−1017.
8. Kleinschmidt, J. H., and Tamm, L. K. (1996) *Biochemistry 35*, 12993−13000.
9. Riede, I., Degen, M., and Henning, U. (1985) *EMBO J. 4*, 2343−2346.
10. Schwarz, H., Riede, I., Sonntag, I., and Henning, U. (1983) *EMBO J. 2*, 375−380.
11. Kay, D., and Fildes, P. (1962) *J. Gen. Microbiol. 27*, 143−146.
12. Kunkel, T. A., Bebenek, K., and McClary, J. (1991) *Methods Enzymol. 204*, 125−139.
13. Raleigh, E. A., Lech, K., and Brent, R. (1989) in *Current Protocols in Molecular Biology* (Ausubel, F. M. E. A., Ed.) Unit 1.4, Publishing Associates and Wiley-Interscience, New York.
14. Yanish-Perron, C., Viera, J., and Messing, J. (1985) *Gene 33*, 103−199.
15. Hanahan, D. (1983) *J. Mol. Biol. 166*, 557−580.
16. Sambrook, J., Fritsch, E. F., and Maniatis, T. (1989) *Molecular Cloning*: *A Laboratory Manual*, Cold Spring Harbor Laboratory, Cold Spring Harbor, NY.
17. Bradford, M. M. (1976) *Anal. Biochem. 72*, 248−254.
18. Morona, R., Krämer, C., and Henning, U. (1985) *J. Bacteriol. 164*, 539−543.
19. McIntosh, T. J., and Holloway, P. W. (1987) *Biochemistry 26*, 1783−1788.
20. Ladokhin, A. S., and Holloway, P. W. (1995) *Biophys. J. 69*, 506−517.
21. Kleinschmidt, J. H., Wiener, M. C., and Tamm, L. K. (1999) (submitted for publication).
22. Freudl, R., Schwarz, H., Stierhof, Y. D., Gamon, K., Hindenach, I., and Henning, U. (1986) *J. Biol. Chem. 261*, 11355−11361.
23. Chen, R., and Henning, U. (1996) *Mol. Microbiol. 19*, 1287−1294.
24. Kahn, T. W., and Engelman, D. M. (1992) *Biochemistry 31*, 6144−6151.
25. Hunt, J., Earnest, T. N., Bousché, O., Kalghatgi, K., Reilly, K., Horváth, C., Rothschild, K. J., and Engelman, D. M. (1997) *Biochemistry 36*, 15156−15176.
26. White, S. H., and Wimley, W. C. (1994) *Curr. Opin. Struct. Biol. 4*, 79−86.
27. Amann, E., Ochs, B., and Abel, K. J. (1988) *Gene 69*, 301−315.